

All-optical optoacoustic microscope based on wideband pulse interferometry

Georg Wissmeyer¹, Dominik Soliman¹, Rami Shnaiderman¹, Amir Rosenthal^{1,2} and Vasilis Ntziachristos^{1*}

¹*Institute for Biological and Medical Imaging & Chair for Biological Imaging
Technische Universität München and Helmholtz Zentrum München*

²*Andrew and Erna Viterbi Faculty of Electrical Engineering,
Technion - Israel Institute of Technology*

*Corresponding author: v.ntziachristos@tum.de

Received Month X, XXXX; revised Month X, XXXX; accepted Month X, XXXX; posted Month X, XXXX (Doc. ID XXXXX); published Month X, XXXX

Optical and optoacoustic (photoacoustic) microscopy have been recently joined in hybrid implementations that resolve extended tissue contrast compared to each modality alone. Nevertheless, the application of the hybrid technique is limited by the requirement to combine an optical objective with ultrasound detection collecting signal from the same micro-volume. We present an all-optical optoacoustic microscope based on a pi-phase-shifted Fiber Bragg Grating (π -FBG) with coherence-restored pulsed interferometry (CRPI) used as the interrogation method. The sensor offers ultra-small footprint and achieved higher sensitivity over piezoelectric transducers of similar size typically employed in intravascular applications. We characterized the spectral bandwidth of the ultrasound detector and interrogated the imaging performance achieved on phantoms and tissues. We discuss the potential uses of all-optical π -FBG sensors based on coherence-restored pulse interferometry.

Optical microscopy plays a critical role in biological and medical applications. Of particular importance for biological research has been the use of fluorescence contrast that allows visualization of cellular and subcellular components. Optoacoustic methods extend high-resolution optical observations beyond the depths reached by optical microscopy and can enable combination of fluorescence and optical absorption contrast [1-4]. The combination of multi-photon microscopy with optoacoustic microscopy has been already demonstrated using a piezoelectric ultrasound detector positioned in transmittance geometry, i.e. on the opposite side of a microscope objective [5]. Optoacoustic microscopy of specimens larger than a few millimeters requires light and sound detection from the same side of the sample, enabling *in-vivo* imaging of standard animal models [6]. The use of piezoelectric transducers may limit however the implementation of optical and optoacoustic microscopy in reflectance mode, due to the physical restrictions of the detection element and surrounding circuitry. Requirements for acoustic focusing, the design of acoustic wave paths, electrical wiring considerations and manufacturing aspects related to the connectorization of the active element impose size specifications that may be incompatible with optical objectives. Moreover, the sensitivity and bandwidth achieved, depend on the area of the active element. Although ultrasound imaging has been achieved with miniaturized piezoelectric detectors, especially in intravascular applications, optoacoustic imaging may require ultrasound detectors of higher sensitivity than the ones employed in classical pulse-echo ultrasound imaging. This is because ultrasound imaging

can adjust the sensitivity by emitting sound of sufficient energy, whereby optoacoustic imaging only relies on sound generation within tissue due to thermoelastic expansion, ultimately limited by photon diffusion and permissible exposure limits for light [1]. An additional limitation of piezoelectric transducers employed in optoacoustic measurements relates to the thermoelastic expansion of the element itself, due to light interfering with the metal casing and active elements of the piezoelectric detector, giving rise to parasitic optoacoustic signals and image artifacts.

Fiber based detectors offer a potent alternative to piezoelectric transducers and have been recently explored for sensing and imaging applications [7,8,9-10]. In this letter, we explore the performance and utility of a pi-phase shifted Fiber Bragg Grating (π -FBG) sensor for ultrasound detection in optoacoustic microscopy. The π -FBG sensor was recently described [11,12]. Its design contains two key characteristics. First, an artificial discontinuity is introduced in a fiber based Bragg Grating. This discontinuity creates a pi-shifted region which is analogous to the cavity of a Fabry-Pérot interferometer (FPI). The transmission spectrum of the device exhibits a characteristic band gap and a narrow transmission notch in its center, attributed to the FPI. In fibers, these cavities exhibit a high finesse and μm scales. Thus, the high Q-factor of the interferometer allows high sensitivity towards pressure variations along the sensor region of the fiber. Second, a wideband pulse interferometer is employed for interrogating the π -FBG sensor. This approach reduces laser noise by coherence restoring pulse interferometry (CRPI) and minimizes optical noise caused

by temperature shifts and vibrations in the low kHz regime by a wideband feedback circuit [13]. By eliminating optical noise, the interrogation system allows to fully exploit the superior sensitivity of the high Q-factor exhibited by the π -FBG sensors.

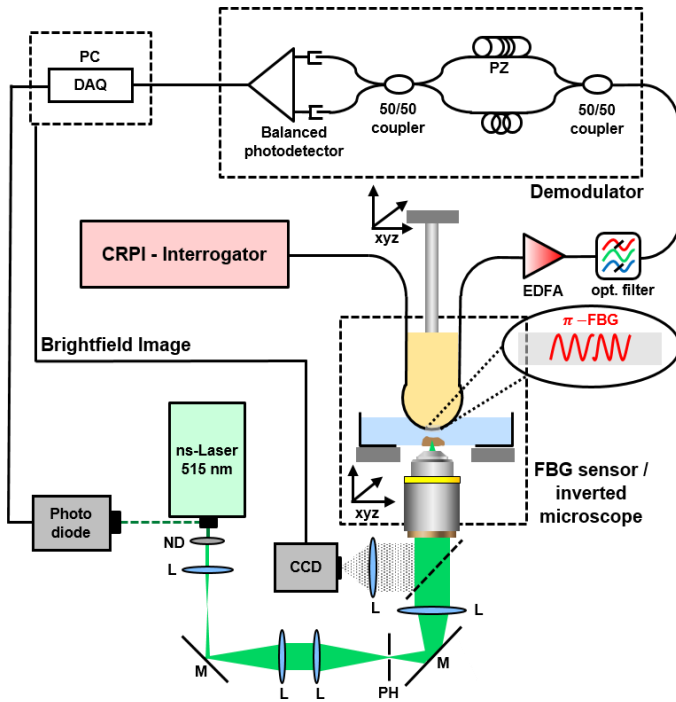


Fig. 1. Schematic of the all-optical optoacoustic microscope. ND, neutral density filter; L, lens; M, mirror; PH, pinhole; xyz, motorized translation stages; DAQ, data acquisition system; EDFA, erbium doped optical amplifier; PZ, piezoelectric fiber stretcher.

The π -FBG sensor is considered herein for integrated miniaturized sensing within an optoacoustic microscopy setup as shown in Fig. 1. Optoacoustic signal excitation was based on a 515 nm DPSS laser (Flare HP PQ Green 2 k-500, Innolight GmbH, Hannover, Germany; 1.8 ns pulse width) generating 570 μ J pulses at a repetition rate of 1.2 kHz. The beam was attenuated and directed to an objective (PLN 10X, NA 0.25, WD 10.6 mm, Olympus, Hamburg, Germany) through a telescope lens, containing a 25 μ m pinhole at the focal spot for spatial light filtering and interfacing. The objective was mounted on a customized inverted microscope (AxioObserver.D1, Zeiss, Jena, Germany) with an embedded CCD camera for bright field imaging (AxioCam ICc 1, Zeiss, Jena, Germany). The laser beam was focused onto a sample placed on a glass bottom petri dish. The petri dish was integrated in a motorized xyz-stage set (xy-stage: MLS203-2 / z-stage: ZMZS500-E, Thorlabs, Newton, NJ, USA; min. step size 0.1 μ m). π -FBG interrogation was based on an ultrafast femtosecond fiber laser with 1550 nm central wavelength and a pulse repetition rate of 250 MHz (Menlo Laser TC-1550 M-comb, Menlo Systems GmbH, Martinsried, Germany). After filtering (0.4 nm bandwidth) and laser pulse amplification, the interrogation laser was directed through a coherence

restoring filter (CRF), similar to the one demonstrated in Ref. [9]. However, in this work, the CRF was implemented with a free-space plano-convex Fabry-Pérot cavity (Optical Frequency Synthesizer, MenloSystems GmbH) with a free spectral range (FSR) of 1 GHz, whereas in Ref. [9] a fiber-based design was used with an FSR of 25 MHz, which limited the effective bandwidth of the detector. A custom made feedback device was applied to lock onto the time-domain comb of the interrogation laser and to control the piezo-mirror in the Fabry-Pérot cavity. The laser light was then directed into the π -FBG sensor (TeraXion Inc., Quebec, Canada). Subsequently, the optoacoustic signal detection is based on ultrasound induced perturbations on the resonator, which cause the transmission notch to shift spectrally and proportionally to the magnitude of the perturbation. Active demodulation in the form of a balanced fiber-based Mach-Zehnder Interferometer (MZI) was used to read out the spectral shifts as a voltage readout from the balanced photo-diode. For imaging, the sample was moved laterally in a discrete manner by means of the motorized xyz-sample-stage and the time-resolved voltage signals were recorded at every position.

To interrogate the bandwidth of the π -FBG sensor we recorded the response of optoacoustic signals generated by 10 μ m diameter black polystyrene microspheres (Polybead, Polysciences, Warrington, FL, USA), with 0.5 μ m step size (Fig. 2c). The Fourier Transform (Fig. 2a) of the collected time-domain signal (Fig. 2b) revealed a peak sensitivity at \sim 20 MHz and an overall bandwidth of 80 MHz. The bandwidth of the system was defined here as the frequency span over which the amplitude exceeds 10% of the maximum value. The locations of apparent resonances in the frequency response depend on the geometry of the fiber based detector and the acoustic impedance matching between water and the coating of the π -FBG sensor [14]. The theoretical bandwidth of the interrogation system is limited by the Nyquist-frequency and is given with 500 MHz. The optical amplifier and the balanced photodiode in the demodulator introduce further restrictions to the theoretical bandwidth in the range of 150 MHz.

The lateral resolution in the experimental setup of Fig. 1 depends on the optical focusing ability of the system and

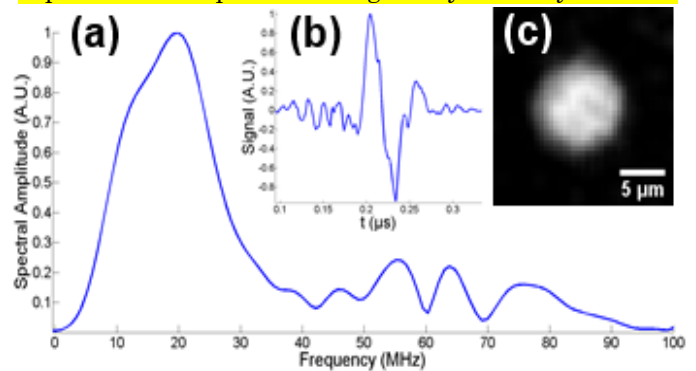


Fig. 2. Characterization of the π -FBG sensor by scanning a 10 μ m black polystyrene sphere (0.5 μ m step size). (a) Frequency response of the CRPI system with the inset (b) showing the corresponding time domain signal recorded at the center of a single sphere. (c) Corresponding maximum intensity projection (MIP).

was set to $\sim 2.2 \mu\text{m}$ [5]. On the other hand, the axial resolution of the optoacoustic microscopy setup depends on the bandwidth of the acoustic detector. To determine the axial resolution, we applied a technique as described in Ref. [5] and found it to be in the order of $12.5 \mu\text{m}$. The π -FBG sensor was installed in a 3d printed and xyz driven (M-683.2, M-501.1, Physik Instrumente, Karlsruhe, Germany) sensor head inside a water tank, as shown in Fig. 1. To examine the ability to utilize this sensor for optoacoustic microscopy we imaged a 10-day-old zebra fish larva and a mouse ear *ex vivo*, together with bright field microscopy. Zebra fish larvae have prominent melanocyte patterns, that absorb strongly in the probed wavelength region (515 nm). The fish was fixated against movement with thin plastic foil and prepared on a glass bottom petri dish with ultrasound gel as sound transmitting medium. Fig. 3(b) shows the maximum intensity projection (MIP) of the recorded optoacoustic signals in a $400 \times 400 \mu\text{m}^2$ region at the trunk of the specimen, indicating a high contrast and a high structural conformity to the corresponding bright field image shown in Fig. 3(a). For potential intravascular applications, it is of particular interest to evaluate optoacoustic imaging of blood and vasculature. For this experiment we examined a mouse ear excised from a mouse immediately after sacrifice. The blood vessels were cauterized to minimize loss of blood and the ear was mounted in the same way as the zebra fish specimen. In Fig. 3(c), the bright field image of the mouse ear sporadically reveals the vasculature, while the optoacoustic MIP in Fig. 3(d) shows a well-defined structure of the vasculature and visualizes parts otherwise indiscernible in the corresponding bright field image.

To elucidate the merits of interferometric detection, we compare the π -FBG sensor to a piezoelectric sensor commonly utilized for intravascular ultrasound (IVUS) detection. We selected a 15 MHz IVUS transducer (Boston Scientific, Boston, MA, USA). The IVUS sensor is based on a piezoelectric element with 1.2 mm diameter and has a sensitivity (noise equivalent pressure) of 1.8 kPa, at 16 MHz bandwidth. The effective sensing area of the fiber based π -FBG sensor has a length of $270 \mu\text{m}$ and a cladding diameter of $125 \mu\text{m}$ [12], while exhibiting a sensitivity of 0.1 kPa. Hence, the sensitivity of the π -FBG sensor is 18 times higher than that of the IVUS sensor despite having a sensing area that is 5.3 times smaller.

In summary, we developed an all-optical optoacoustic microscope by implementing a pi-phase shifted fiber Bragg grating based ultrasound detector into an optical-resolution optoacoustic microscopy modality. With the demonstrated system, high-resolution images of *ex vivo* mouse ear and zebra fish larva were produced of a quality that is on par with optoacoustic images generated with sophisticated focused piezoelectric transducers [6,15]. This can be attributed to the high sensitivity and wide bandwidth of the detector. Moreover, its side-looking and cylindrically symmetric geometry make it attractive for other biomedical applications where small footprints are of importance, e.g. in intravascular and *in-vivo* optoacoustic imaging of large specimen. Furthermore, in modalities where the sensor is exposed to electromagnetic disturbances, the all-optical nature of the π -FBG sensor

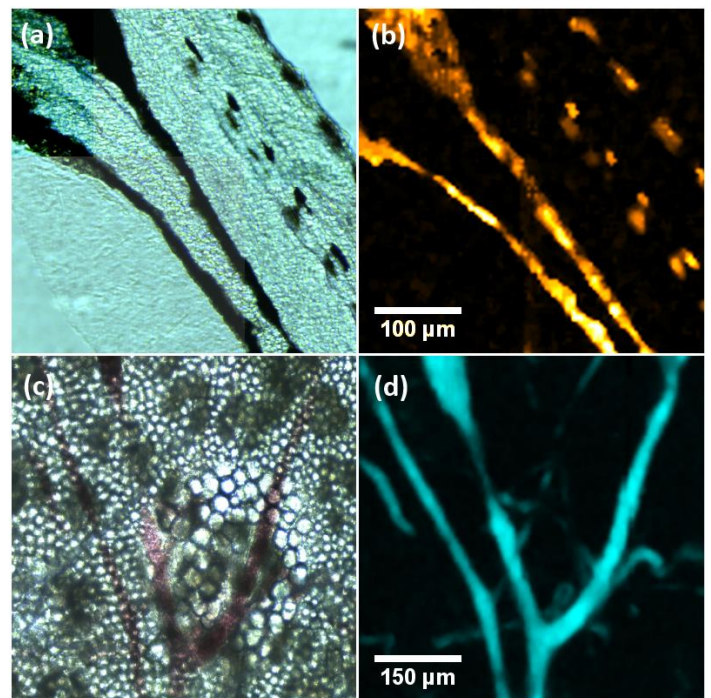


Fig. 3. Microscopy scans of a zebra fish larva (a-b) and a mouse ear (c-d) *ex vivo*. (a) Bright field and (b) CRPI based optoacoustic MIP of a $400 \times 400 \mu\text{m}^2$ region at the trunk of the zebra fish, showing melanocytes. (c) Bright field and (d) optoacoustic MIP of a mouse ear showing the ear vasculature in the same $600 \times 600 \mu\text{m}^2$ FOV.

could represent a major advantage.

The system could be further improved, e.g. by using acoustically matched materials to avoid coupling losses or by applying multiplexing techniques to simultaneously interrogate multiple sensors. Overall, the performance of the demonstrated ultrasound detector implemented in the optoacoustic microscope, along with its ultra-small dimensions, underline the potential to supplement or replace existing piezoelectric transducers.

G. Wissmeyer and A. Rosenthal acknowledge the support from the German Research Foundation (DFG) Research Grant (RO 4268/4-1) and the CRC 1123 (Z1).

V. Ntziachristos acknowledges the support from the European Research Council through an Advanced Investigator Award.

References

1. V. Ntziachristos, Nat. Methods **7**, 603 (2010).
2. F. Helmchen and W. Denk, Nat. Methods **2**, 932 (2005).
3. A. Taruttis and V. Ntziachristos, Nat. Photonics **9**, 219 (2015).
4. L. V. Wang and S. Hu, Science **335**, 1458 (2012).
5. D. Soliman, G.J. Tserevelakis, M. Omar and V. Ntziachristos, Sci. Rep. **5**, (2015).
6. S. Hu, K. Maslov and L. V. Wang, Med. Phys. Lett. **36**, 2320 (2009).
7. P. Morris, A. Hurrell, A. Shaw, E. Zhang and P. Beard, J. Acoust. Soc. Am. **125**, 3611 (2009).

8. J. Haller, V. Wilkens, K.-V. Jenderka, C. Koch, J. Acoust. Soc. Am. **129**, 3676 (2011).
9. A. Rosenthal, S. Kellnberger, D. Bozhko, A. Chekkoury, M. Omar, D. Razansky and V. Ntziachristos, Laser Phot. Rev. **49**, 1 (2014).
10. D. Gallego and H. Lamela, Opt. Lett. **34**, 1807 (2009).
11. A. Rosenthal, D. Razansky and V. Ntziachristos, Opt. Lett. **36**, 1833 (2011).
12. A. Rosenthal, M. Á. A. Caballero, S. Kellnberger, D. Razansky, and V. Ntziachristos, Opt. Lett. **37**, 3174 (2012).
13. A. Rosenthal, S. Kellnberger, G. Sergiadis, and V. Ntziachristos, IEEE Photonics Technol. Lett. **24**, 1499 (2012).
14. V. István, P. Burgholzer, T. Berer, A. Rosenthal, G. Wissmeyer and V. Ntziachristos, JASA **135**, 1853 (2014).
15. G. J. Tserevelakis, D. Soliman, M. Omar and V. Ntziachristos, Opt. Lett. **39**, 1819 (2014).